# Electronic Supplementary Information

**Uniformly-distributed Sb nanoparticles in ionic liquid-derived nitrogen-enriched carbon for highly reversible sodium storage**

*Xin Xu,[a] Zhifeng Dou,[b] Erlong Gu,[a] Ling Si,[a] Xiaosi Zhou*[a] and Jianchun Bao*[a]*

[a] Jiangsu Key Laboratory of New Power Batteries, Jiangsu Collaborative Innovation Center of Biomedical Functional Materials, School of Chemistry and Materials Science, Nanjing Normal University, Nanjing 210023, P. R. China

*E-mail: zhouxiaosi@njnu.edu.cn

*E-mail: baojianchun@njnu.edu.cn

[b] State Key Lab of Marine Resource Utilization in South China Sea, College of Materials and Chemical Engineering, Hainan University, Haikou 570228, P. R. China

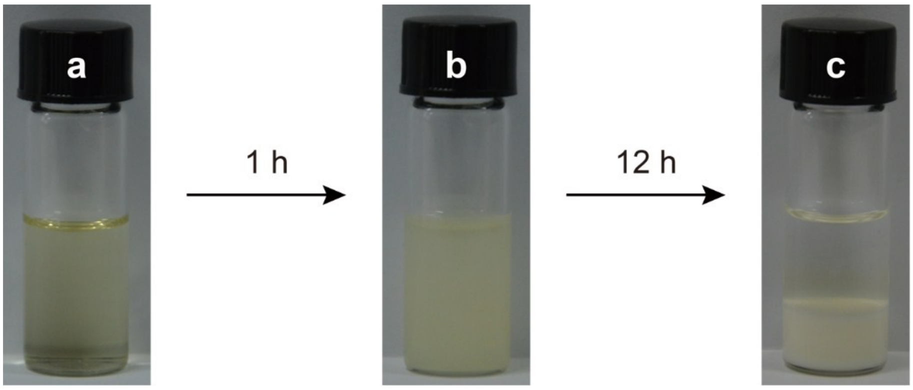


**Fig. S1** Digital photographs of (a) a mixture prepared by mixing 3 mL of $SbCl_3$/methanol (80 mg $mL^{-1}$) solution and 3 mL of Emim-dca/methanol (100 mg $mL^{-1}$) solution and the mixture after depositing for (b) 1 h and (c) 12 h.

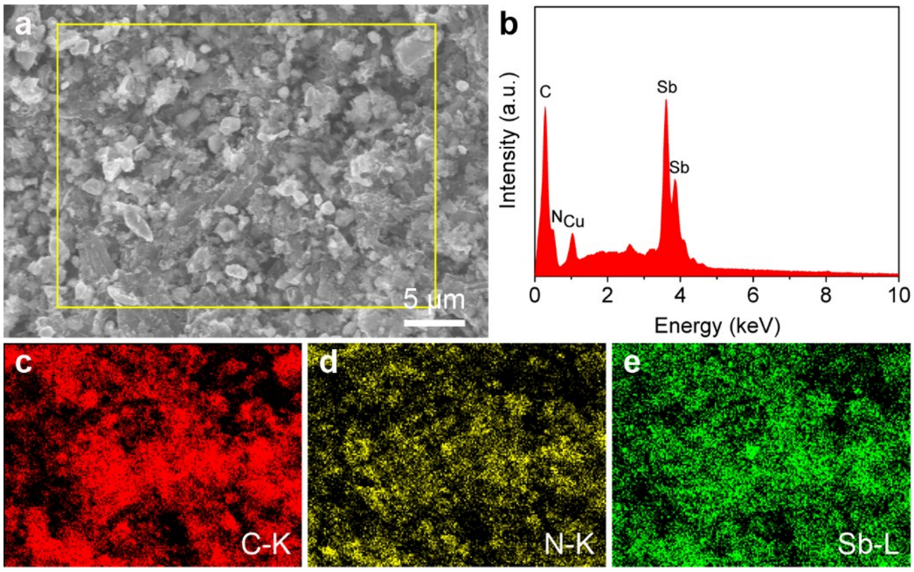


**Fig. S2** (a) SEM image and (b−e) corresponding EDX spectrum and C, N, and Sb elemental mapping images of Sb@NC.

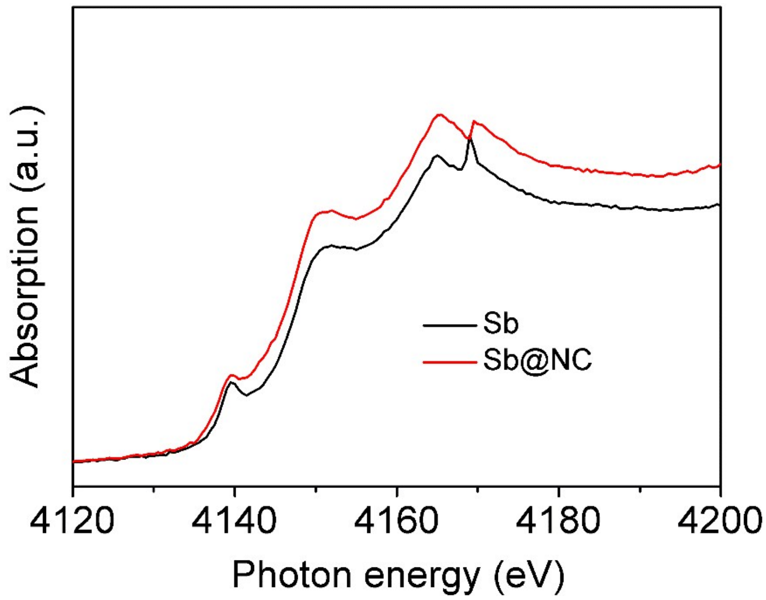


**Fig. S3** Sb $L_3$-edge XANES of Sb and Sb@NC.

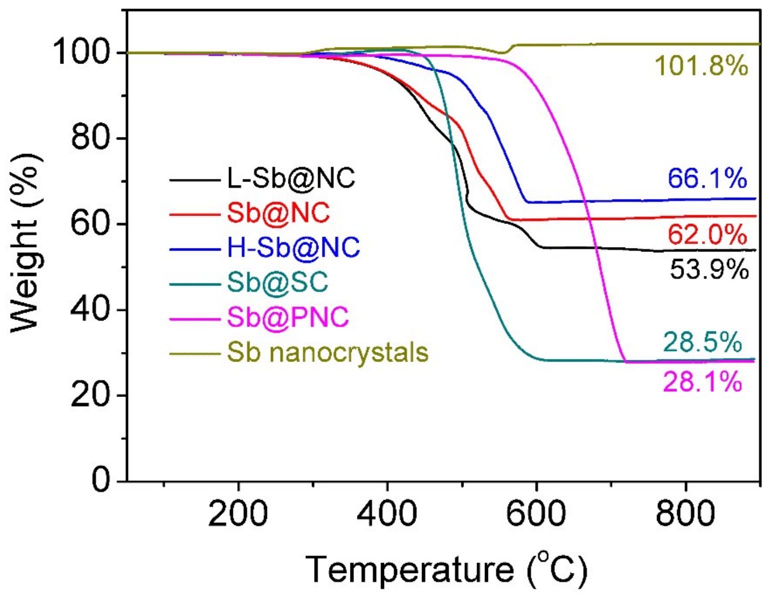


**Fig. S4** TGA of L-Sb@NC, Sb@NC, H-Sb@NC, Sb@SC, Sb@PNC, and Sb nanocrystals under an air flow with a temperature ramp of 10 °C min$^{-1}$ from room temperature to 900 °C. From the TGA curve of Sb nanocrystals, we can clearly see that the weight of Sb nanocrystals remains almost unchanged. This is mainly because Sb nanocrystals experience weight gain due to oxidation and suffer from weight loss owing to heat evaporation at the same time. Therefore, when we calculate the Sb contents in the samples through TGA, only the combustion loss of carbon matrix is taken into account and the weight variation of Sb is ignored.

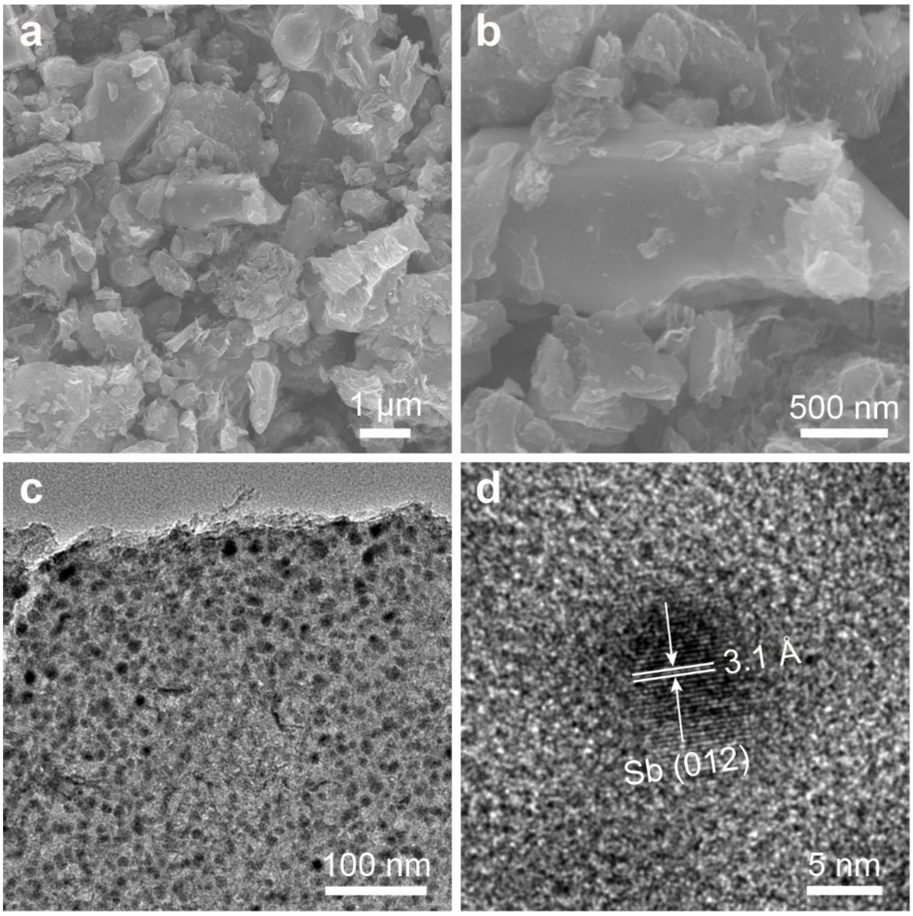


**Fig. S5** (a) SEM image, (b) high-magnification SEM image, (c) TEM image, and (d) HRTEM image of L-Sb@NC.

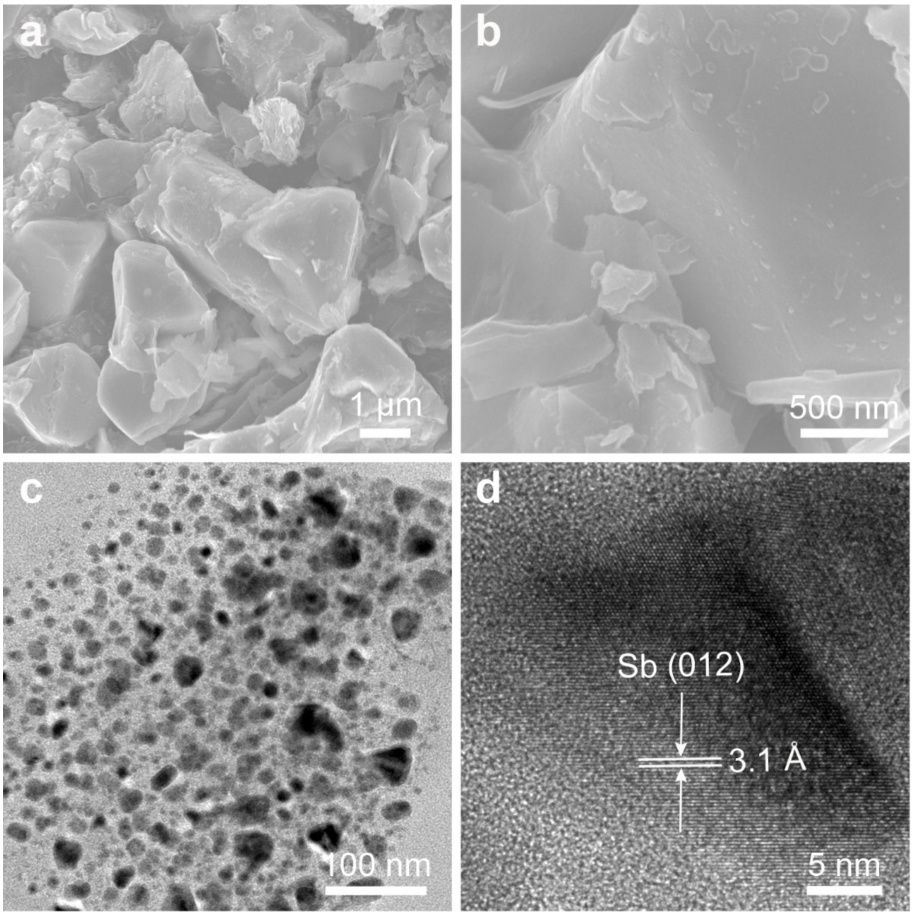


**Fig. S6** (a) SEM image, (b) high-magnification SEM image, (c) TEM image, and (d) HRTEM image of H-Sb@NC.

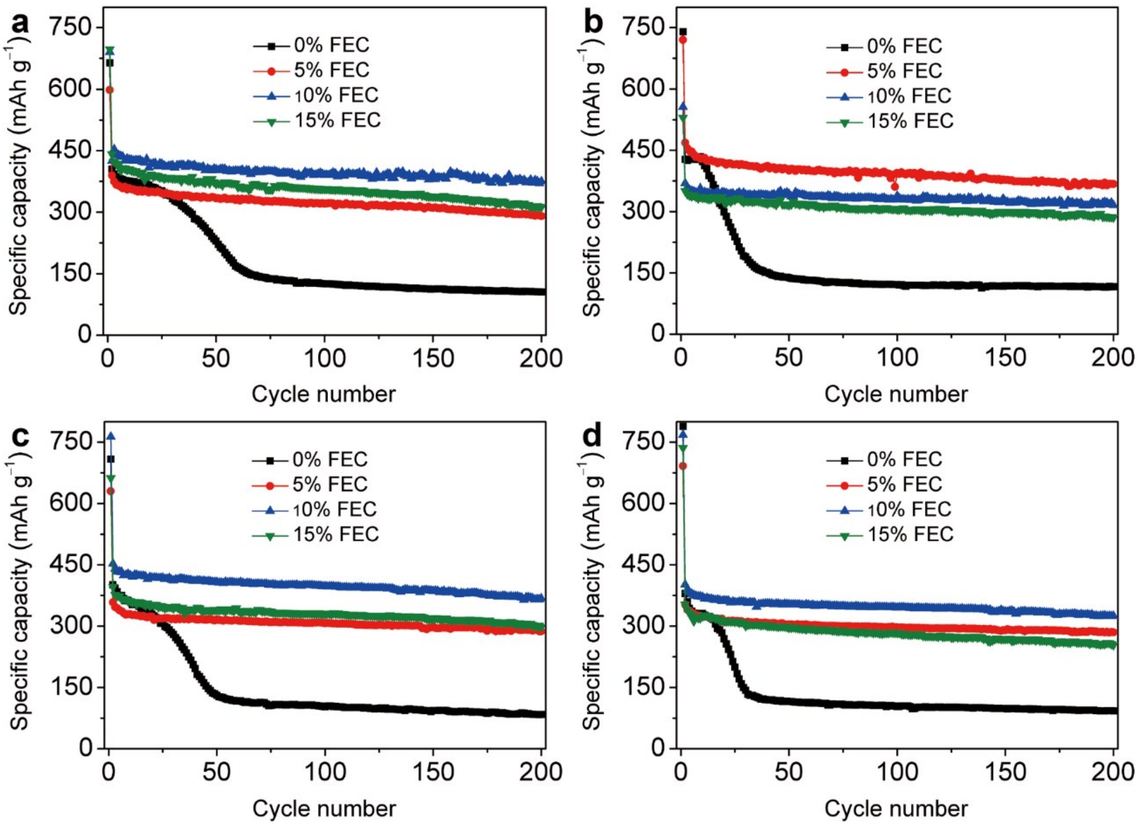


**Fig. S7** (a) The effect of FEC on the electrochemical performance of Sb@NC using 1 M $NaClO_4$ in EC/DEC (1:1 v/v). (b) The effect of FEC on the electrochemical performance of Sb@NC using 1 M $NaClO_4$ in PC. (c) The effect of FEC on the electrochemical performance of Sb@NC using 0.6 M $NaPF_6$ in EC/DEC (1:1 v/v). (d) The effect of FEC on the electrochemical performance of Sb@NC using 1 M $NaPF_6$ in PC. All these investigations were conducted between 0.01 and 2 V at a current density of 100 mA $g^{-1}$.

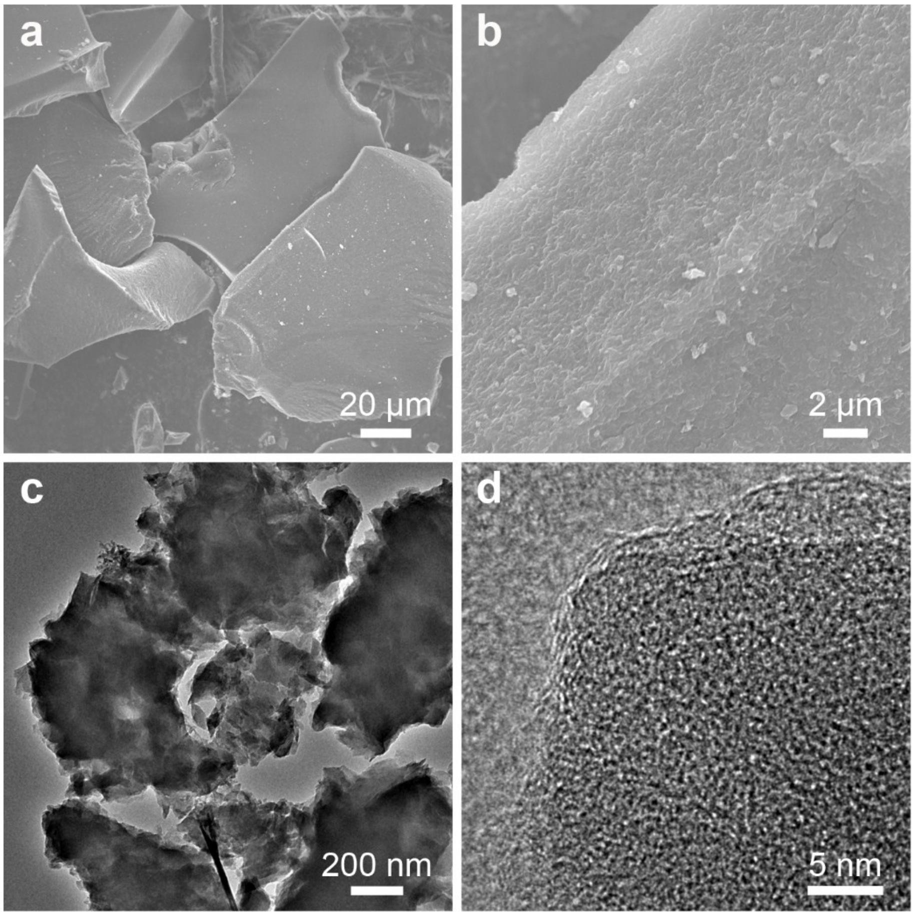


**Fig. S8** (a) SEM image, (b) high-magnification SEM image, (c) TEM image, and (d) HRTEM image of NC.

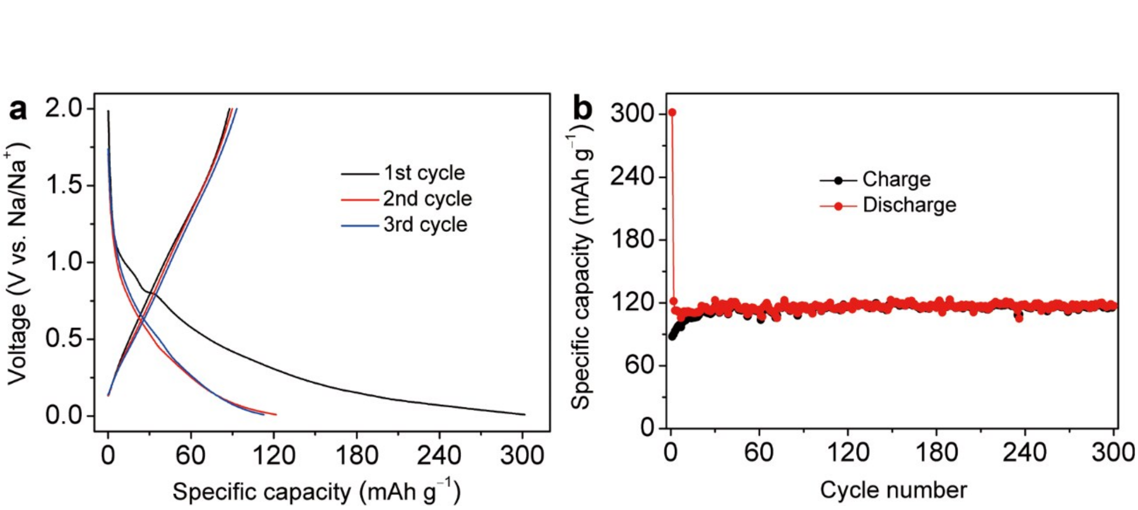

**Fig. S9** Electrochemical properties of the NC anode for sodium-ion batteries. (a) The galvanostatic discharge−charge profiles of the initial three cycles for the NC electrode between 0.01 and 2 V at a current density of 100 mA $g^{-1}$. (b) Discharge−charge capacities for the first 300 cycles of the NC electrode in the voltage range of 0.01−2 V at 100 mA $g^{-1}$.

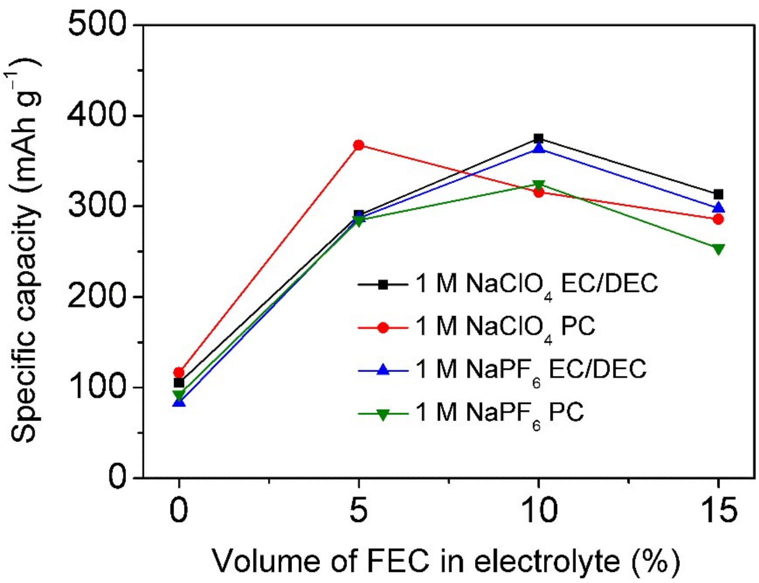


**Fig. S10** The influence of FEC in different electrolytes on the electrochemical properties of Sb@NC. The discharge capacities of the 200th cycle were used for comparison. All these battery tests were performed between 0.01 and 2 V at a current density of 100 mA $g^{-1}$.

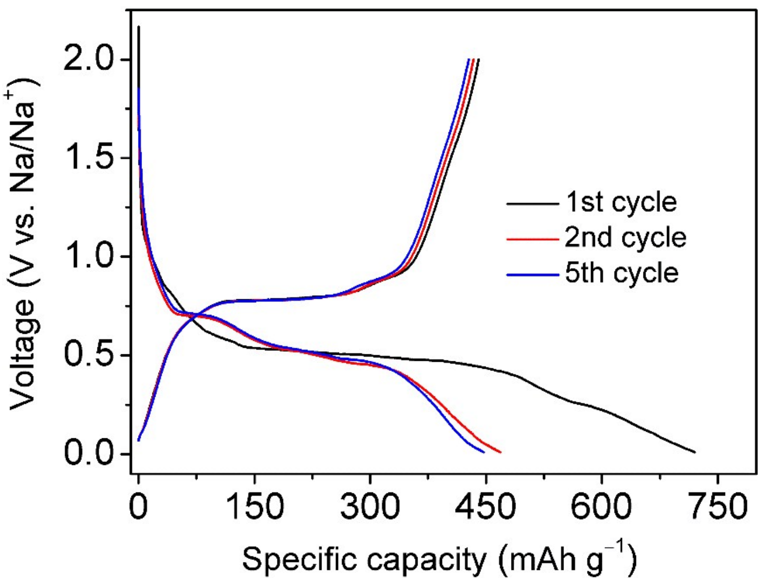


**Fig. S11** Galvanostatic discharge–charge profiles of the Sb@NC electrode plotted for the 1st, 2nd, and 5th cycles between 0.01 and 2 V at a current density of 100 mA $g^{-1}$.

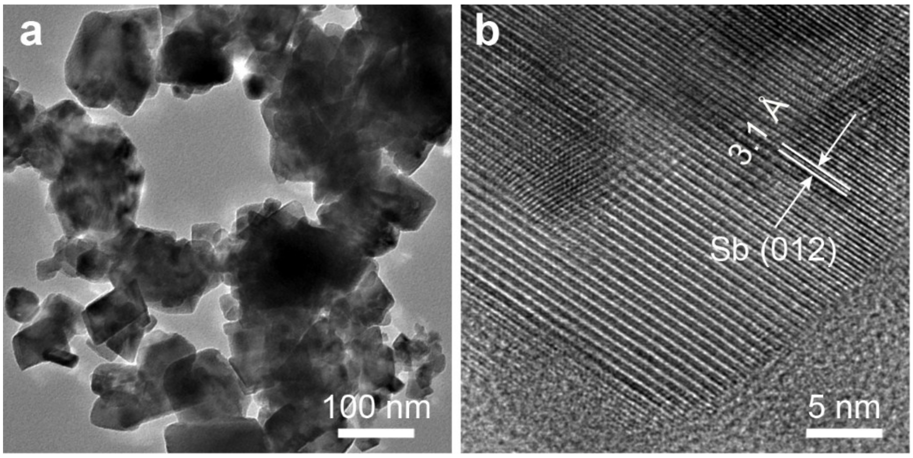


**Fig. S12** (a) TEM image and (b) HRTEM image of Sb nanocrystals.

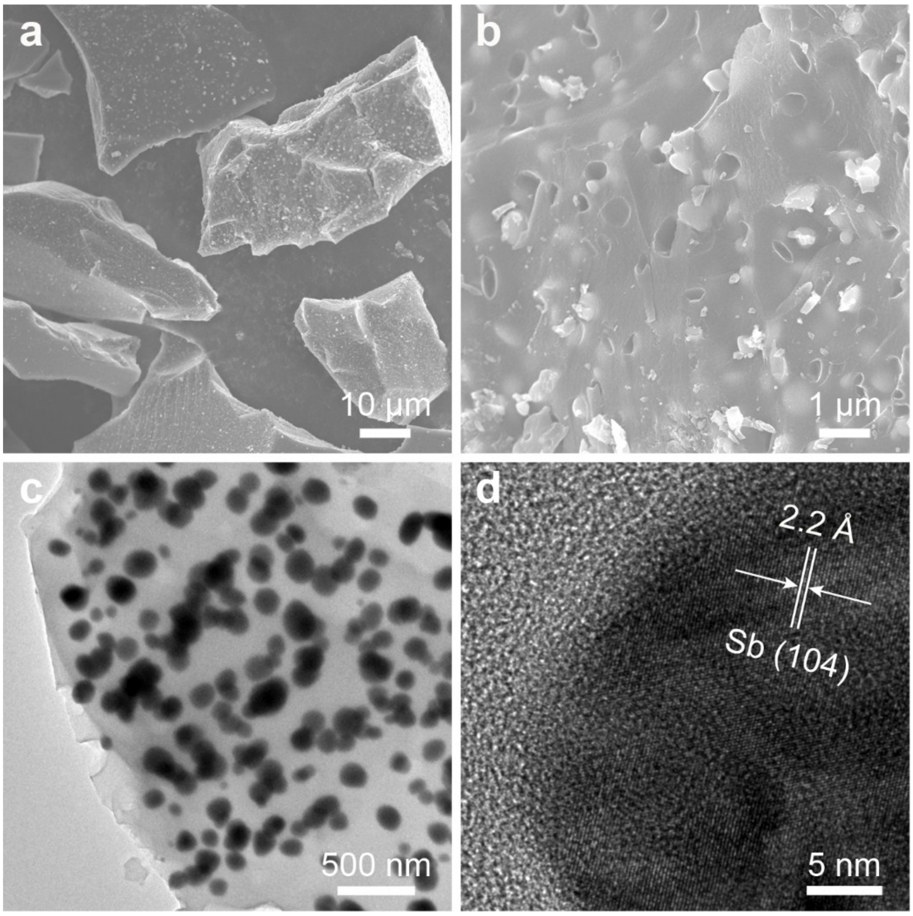


**Fig. S13** (a) SEM image, (b) high-magnification SEM image, (c) TEM image, and (d) HRTEM image of Sb@SC.

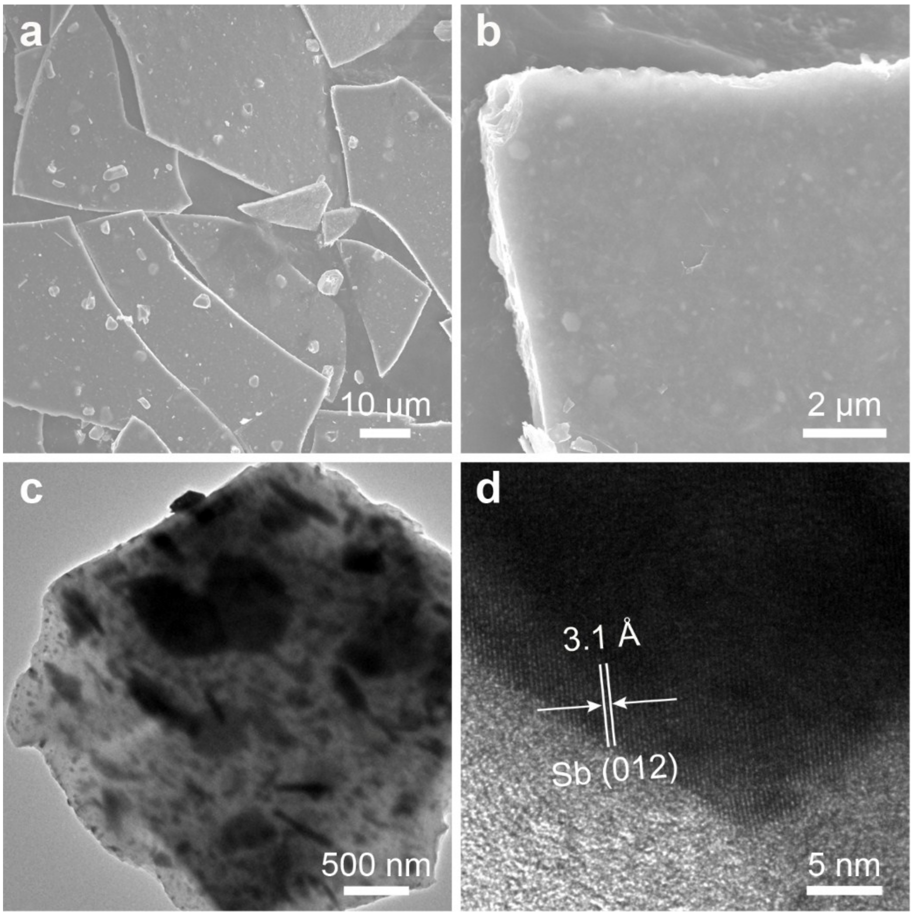


**Fig. S14** (a) SEM image, (b) high-magnification SEM image, (c) TEM image, and (d) HRTEM image of Sb@PNC.

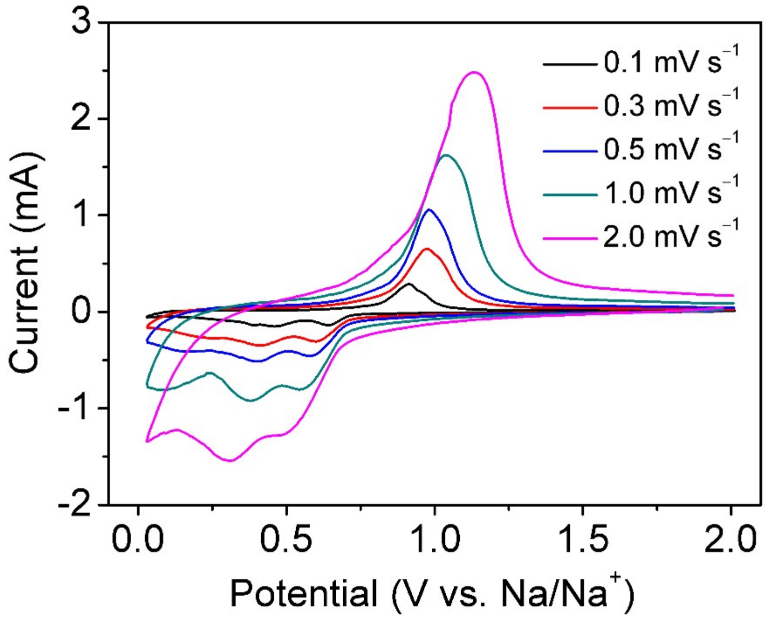


**Fig. S15** CV curves of the Sb@NC electrode at different scan rates.

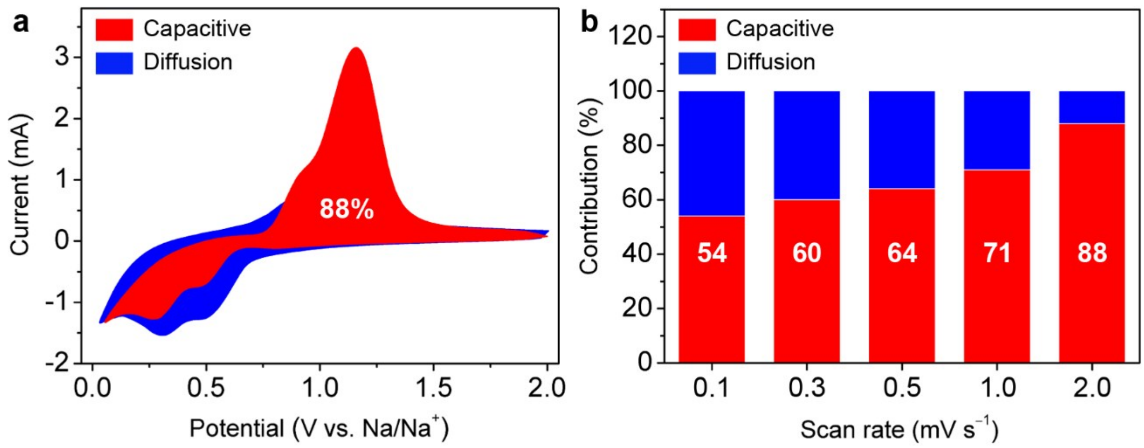


**Fig. S16** Kinetics and quantitative analysis of sodium storage mechanism. (a) Capacitive (red) and diffusion-dominated (blue) contribution to sodium storage of Sb@NC at 2.0 mV $s^{-1}$. (b) Normalized contribution ratio of capacitive (red) and diffusion-limited (blue) capacities at various scan rates.

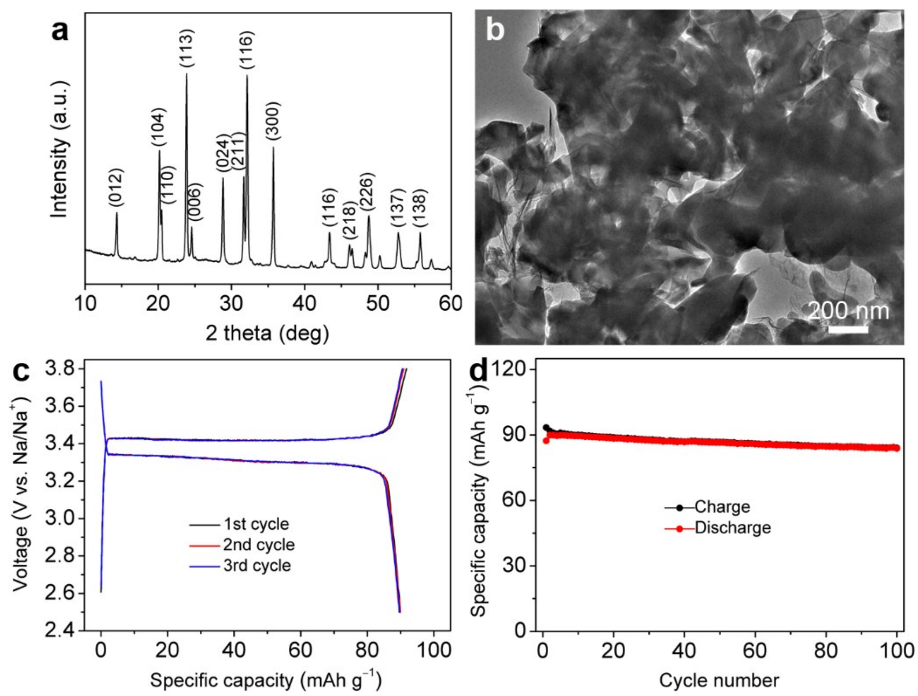


**Fig. S17** (a) XRD pattern, (b) TEM image, (c) discharge−charge curves, and (d) cycling performance of the $Na_3V_2(PO_4)_3/C$ cathode between 2.5 and 3.8 V at a current density of 100 mA $g^{-1}$.

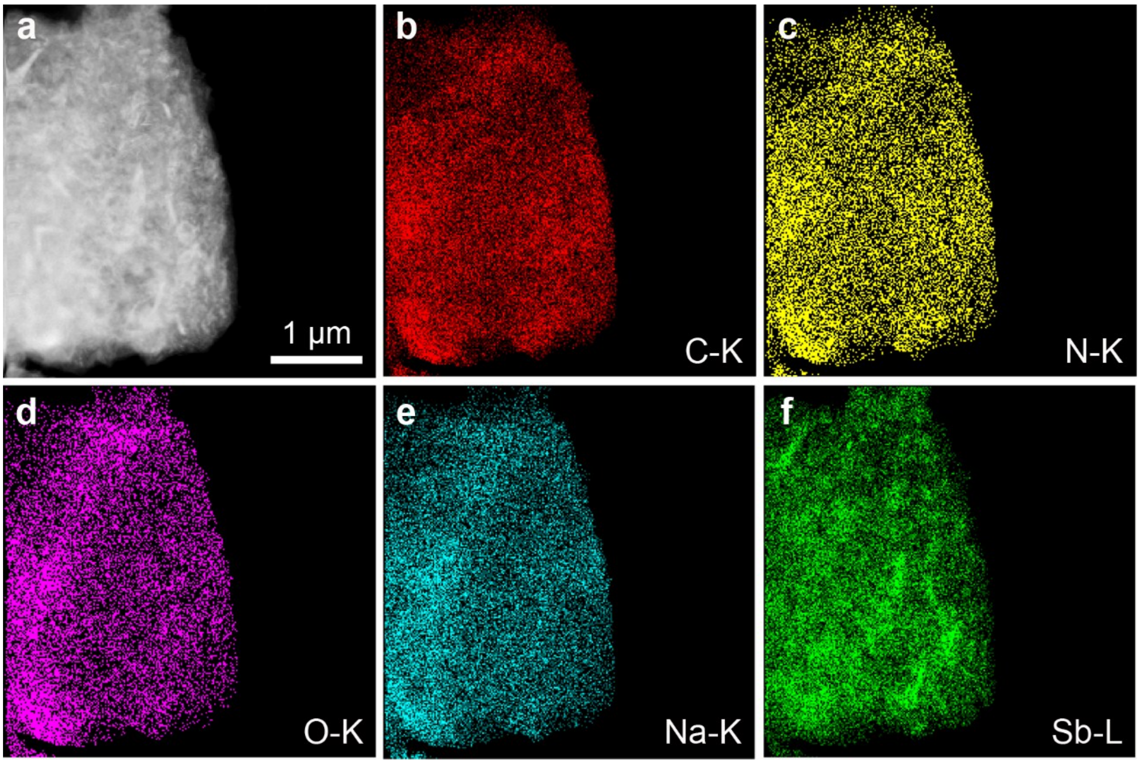


**Fig. S18** STEM and EDX elemental mapping images of the Sb@NC electrode material after cycling 300 cycles between 0.01 and 2 V at a current density of 100 mA $g^{-1}$.

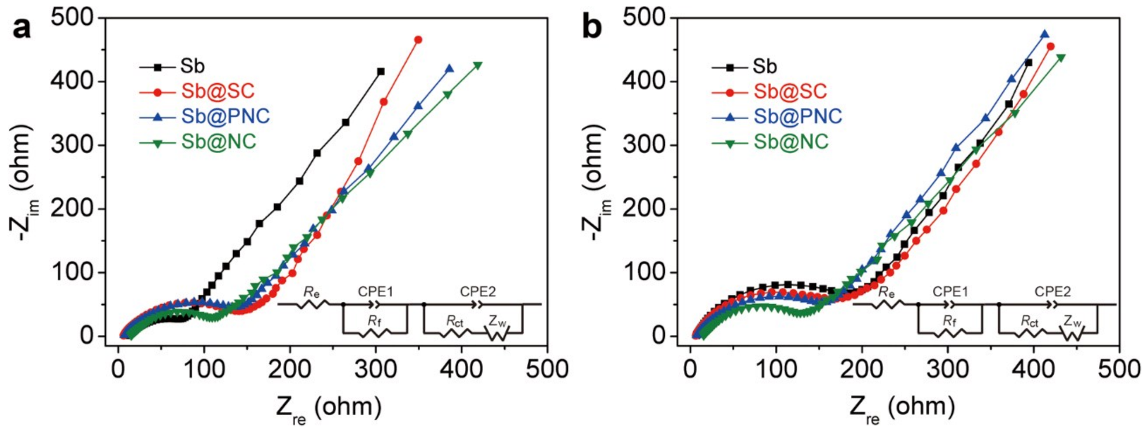


**Fig. S19** Nyquist plots for the Sb, Sb@SC, Sb@PNC, Sb@NC cells (a) after the first cycle and (b) after 5 cycles acquired by using a sine wave with an amplitude of 10.0 mV over the frequency range of 100 kHz−100 mHz. The insets show the equivalent circuits applied for data fitting. $R_e$, $R_f$, and $R_{ct}$ represent electrolyte resistance, SEI film resistance, and charge-transfer resistance, respectively. CPE1 and CPE2 are the abbreviation of the constant phase elements, usually corresponding to the SEI film capacitance and the double-layer capacitance, respectively. $Z_w$ is the Warburg impedance, commonly ascribed to the diffusion of sodium ions into the bulk electrodes.

**Table S1.** Kinetic parameters of the Sb, Sb@SC, Sb@PNC, Sb@NC cells after different cycles.

| Sample | $R_e$ (after 1 cycle) | $R_f$ (after 1 cycle) | $R_{ct}$ (after 1 cycle) | $R_e$ (after 5 cycles) | $R_f$ (after 5 cycles) | $R_{ct}$ (after 5 cycles) |
|---|---|---|---|---|---|---|
| Sb | 13.0 | 62.8 | 0.01 | 9.3 | 188.2 | 0.01 |
| Sb@SC | 8.2 | 144.1 | 0.01 | 8.4 | 186.4 | 0.01 |
| Sb@PNC | 10.0 | 117.8 | 0.01 | 9.3 | 123.5 | 0.01 |
| Sb@NC | 9.1 | 92.1 | 0.01 | 9.3 | 95.4 | 0.01 |

**Table S2.** A survey of nitrogen contents in electrode materials.

| Electrode material | Synthetic method | Nitrogen content | Reference |
|---|---|---|---|
| Ionic liquid-derived nitrogen-enriched carbon | Pyrolysis of Emim-dca | 16.86 wt% | This work |
| Nitrogen-doped carbon sheets | Carbonization of okara | 9.89 at.% | 1 |
| Nitrogen-doped carbon nanofiber film | Carbonization of PI nanofiber film | 7.15 wt% | 2 |
| Highly crumpled nitrogen-doped graphene sheets | Thermally induced expansion of the mixture of GO and cyanamide | 6.53 wt% | 3 |
| Nitrogen-doped mesoporous hollow carbon spheres | Chemical vapor deposition | 7.5 at.% | 4 |
| ZIF-8 derived carbon polyhedrons | Carbonization of ZIF-8 | 18.7 wt% | 5 |
| Nitrogen-doped activated carbons | Heat treatment of corncobs | ~4 wt% | 6 |
| Nitrogen-doped porous interconnected doubled-shelled hollow carbon spheres | Chemical treatment of $Fe_3O_4$@polyacrylamide-derived carbon | 2.17 wt% | 7 |
| 3D N-doped graphene foams | Annealing the freeze-dried graphene oxide foams in ammonia | 6.8 at.% | 8 |
| Highly nitrogen-doped porous carbon | Pyrolysis of a nitrogen-containing zeolitic imidazolate | 17.72 wt% | 9 |
| Graphitic carbon nitride nanosheet−carbon nanotube porous composite | Low-temperature self-assembly | 23.7 wt% | 10 |
| N-doped CNTs | Thermally treated under Ar/$NH_3$ at 1100 $^{o}$C | 3.56 at.% | 11 |
| Mesoporous nitrogen-rich carbon | Pyrolysis of protein | 7.11 wt% | 12 |
| N-doped carbon coating | Carbonization of polydopamine | 14.16 wt%[a] | 13 |
| Nitrogen-doped graphene | Thermal annealing the mixture of melamine and GO | 10.1 at.% | 14 |
| Nitrogen-doped carbon nanotube | Aerosol-assistant catalytic chemical vapor deposition | 2.89 at.% | 15 |

[a] The nitrogen content is calculated based on the mass of N-doped carbon in the $Fe_3O_4$@NC composite.

**Table S3.** Electrochemical performances of Sb-based anode material in SIBs.

| Active material | Voltage range (V vs. $Na/Na^+$) | Mass loading ($mg\ cm^{-2}$) | Composition (wt%) | Current density ($mA\ g^{-1}$) | Reversible capacity ($mAh\ g^{-1}$) | Reference |
|---|---|---|---|---|---|---|
| Sb@NC | 0.01−2 | 0.8−1.2 | Sb: 62.0<br>C: 38.0 | 100 | 395 (after 100 cycles) [a] | This work |
| Sb@NC | 0.01−2 | 0.8−1.2 | Sb: 62.0<br>C: 38.0 | 100 | 565 (after 100 cycles) [b] | This work |
| Sb@NC | 0.01−2 | 0.8−1.2 | Sb: 62.0<br>C: 38.0 | 100 | 328 (after 300 cycles) [a] | This work |
| Hollow Sb@C yolk−shell nanospheres | 0.01−2.6 | Not reported | Sb: 82.4<br>C: 17.6 | 1000 | 280 (after 200 cycles) [a] | 16 |
| Sb/porous carbon nanocomposites | 0.01−2.0 | 0.8−1.1 | Sb: 64.15<br>C: 35.85 | 100 | 523 (after 250 cycles) [b] | 17 |
| $Cu_2Sb$ | 0.05−2 | 0.6 $mg\ cm^{-2}$ | Sb: 48.9<br>Cu: 51.1 | 800 | 256 (after 200 cycles) [c] | 18 |
| Sb-$AlC_{0.75}$-C composite | 0−2.0 | Not reported | Sb: 63<br>$AlC_{0.75}$-C: 37 | 100 | 243 (after 100 cycles) [a] | 19 |
| Sb−CNC hybrid | 0 −2 | ~1.0 | Sb: 66.5<br>C: 33.5 | 100 | 439 (after 150 cycles) [a] | 20 |
| Zn-Sb nanowires | 0.01−2.0 | 1.0 | $Zn_4Sb_3$: 100 | 414 | 298 (after 200 cycles) [c] | 21 |
| Sb/cross-linked chitosan as polymer binder | 0.01−2.0 | ~1.0 | Sb: 100 | 600 | 463 (after 100 cycles) [b] | 22 |
| NP-Sb70 | 0.1−1.5 | Not reported | Sb: 100 | 100 | 574 (after 200 cycles) [b] | 23 |
| Sb@$TiO_{2-x}$ Nanotubes | Not reported | 1−1.5 | Sb: 75<br>$TiO_{2-x}$: 25 | 660 | 547 (after 120 cycles) [a] | 24 |
| Sb@C coaxial nanotubes | 0.01−2.0 | ~0.9 | Sb: 60.9<br>C: 39.1 | 150 | 407 (after 240 cycles) [a] | 25 |
| Sb/N-carbon+CNTs | 0.01−2 | 1.0−1.2 | Sb: 64<br>C: 36 | 100 | 543 (after 200 cycles) [a] | 26 |
| Sb@C microspheres | 0.01−2.0 | ~2.5 | Sb: 41<br>C: 59 | 180 | 456 (after 300 cycles) [b] | 27 |
| SbNPs@3D-C | 0.01−3 | Not reported | Sb: 31.2<br>C: 68.8 | 100 | 430 (after 500 cycles) [a] | 28 |
| Sb/C/G nanocomposite | 0.01−2 | ~2.5 | Sb: 41.8<br>C: 58.2 | 125 | 428 (after 300 cycles) [b] | 29 |
| Sb-O-G | 0.01−2 | 2−3 | Sb: 53 | 250 | 460 (after 200 | 30 |

| | | | | | | |
|---|---|---|---|---|---|---|
| micro/nanomaterial | | | C: 47 | | cycles) [a] | |
| SiC–Sb–C composite | 0.01−2.0 | ~2 | Sb: 70<br>SiC-C: 30 | 100 | 492 (after 100 cycles) [a] | 31 |
| I-Sb/rGO composite | 0.1−2.0 | ~2 | Sb: 53<br>C: 47 | 500 | 173 (after 150 cycles) [a] | 32 |
| Nano-Sb@C composite | 0.01−2.0 | ~0.8 | Sb: 68.8<br>C: 31.2 | 100 | 385 (after 500 cycles) [a] | 33 |
| $Bi_{0.57}Sb_{0.43}$-C | 0.05−2 | ~2 | Bi-Sb: 83.4<br>C: 16.6 | 100 | 375 (after 50 cycles) [a] | 34 |
| G@NiSb/Sb@NF | 0.01−2.0 | 1.26 | Sb: 5.5<br>C: 0.15 | 200 | 340 (after 50 cycles) [a] | 35 |
| Sb PHMSs | 0.01−2 | 1.0−1.2 | Sb: 100 | 100 | 617 (after 100 cycles) [b] | 36 |
| Sb nanorod arrays | 0.01−2.0 | ~0.4 | Sb: 100 | 200 | 521 (after 250 cycles) [b] | 37 |
| Sb/$C_{CHI}$ nanocomposite | 0.01−2.0 | ~2 | Sb: 40.9<br>C: 59.1 | 500 | 372 (after 100 cycles) [a] | 38 |
| Sb/ICNNs composite | 0.01−2 | Not reported | Sb: 80.8<br>C: 19.2 | 100 | 542 (after 100 cycles) [a] | 39 |
| Sb/MLG hybrid | 0.01−2 | 1.0−1.5 | Sb: ~40<br>C: ~60 | 100 | 406 (after 200 cycles) [a] | 40 |
| Sb@3D RCN | 0.01−2.8 | ~0.7 | Sb: 68<br>C: 32 | 132 | 404 (after 100 cycles) [a] | 41 |
| Pitaya-like Sb@C microspheres | 0.01−2.0 | Not reported | Sb: 40.8<br>C: 59.2 | 44 | 609 (after 100 cycles) [b] | 42 |
| Sb@S,N-3DPC | 0.001−2.0 | ~0.7 | Sb: 56<br>C: 44 | 100 | 451 (after 500 cycles) [a] | 43 |
| Sb/rGO paper | 0.01−2.0 | ~0.25 | Sb: 35.3<br>C: 64.7 | 1000 | 467 (after 100 cycles) [a] | 44 |
| Sb NCs | 0.02−1.5 | ~0.5 | Sb: 100 | 660 | 550 (after 250 cycles) [b] | 45 |
| $Sb_2S_3$-graphite | 0.01−2.8 | 1.5 mg/electrode | $Sb_2S_3$: 80<br>C: 20 | 1000 | 656 (after 100 cycles) [a] | 46 |
| Sb-C-G composite | 0.01−2.0 | Not reported | Sb: 15.1<br>C: 84.9 | 100 | 274 (after 100 cycles) [a] | 47 |
| CL-Sb | 0.01−2.00 | 1.0−1.2 mg/electrode | Sb: 100 | 100 | 629 (after 120 cycles) [b] | 48 |
| Sb/$Sb_2O_3$−PPy | 0.001−1.5 | 0.67 | Sb/$Sb_2O_3$:93.3<br>C: 2.7 | 66 | 512 (after 100 cycles) [b] | 49 |
| RGO-SnSb nanocomposite | 0.001−2.5 | Not reported | Not reported | 100 | 361 (after 80 cycles) [a] | 50 |
| NiSb hollow nanospheres | 0.01−2.0 | Not reported | NiSb: 100 | 60 | 500 (after 70 cycles) [c] | 51 |

| | | | | | | |
|---|---|---|---|---|---|---|
| ZnSb/C composite | 0.0−2.0 | Not reported | Not reported | 50 | 301 (after 30 cycles) [a] | 52 |
| $SbO_x$/RGO | 0−2 | ~1.5 | Sb: ~75 C: ~25 | 1000 | 409 (after 100 cycles) [a] | 53 |
| Sb−carbon composite | 0.001−2 | Not reported | Sb: ~46 C: ~54 | 300 | 372 (after 100 cycles) [a] | 54 |
| Sb–C nanofibers | 0.01−2.0 | ~0.7 | Sb: 38 C: 62 | 200 | 446 (after 400 cycles) [b] | 55 |
| Sb/G | 0.005−2.0 | Not reported | Sb: 84.1 C: 15.9 | 20 | 211 (after 30 cycles) [a] | 56 |
| Sb–N/C composite | 0.01−3.00 | 1.0–2.0 | Sb: 15.6 C: 84.4 | 50 | 305 (after 60 cycles) [a] | 57 |
| 20 nm Sb nanocrystals | 0.02−1.5 | ~1.0 | Sb: 100 | 660 | ~580 (after 100 cycles) [b] | 58 |
| CNF-SnSb | 0.0001−2.0 | 1.5–2.0 | SnSb: ~60 C: ~40 | 100 | 345 (after 205 cycles) [a] | 59 |
| Sn−Ge−Sb alloys | 0.01−2 | Not reported | Sb: 28.2 Sn: 55.0 Ge: 16.8 | 85 | 656 (after 50 cycles) [c] | 60 |
| Sb/MWCNT nanocomposite | 0−2 | 1.0–1.2 | Sb: 75.3 C: 24.7 | 200 | 382 (after 120 cycles) [a] | 61 |
| rGO/$Sb_2S_3$ | 0−2 | ~1.0 | $Sb_2S_3$: 83 C: 17 | 50 | 670 (after 50 cycles) [a] | 62 |
| SbNP@C | 0−2 | 3.0 mg/electrode | Sb: 54 C: 46 | 100 | 350 (after 300 cycles) [a] | 63 |
| SiC−Sb−C nanocomposites | 0.01−2.0 | Not reported | Sb: 70 SiC−C: 20 | 100 | 480 (after 50 cycles) [a] | 64 |
| Sb/C nanocomposite | 0−2 | ~3.0 | Sb: 70 C: 30 | 100 | 575 (after 100 cycles) [b] | 65 |
| SnSb/C nanocomposite | 0−1.2 | Not reported | SnSb: 70 C: 30 | 100 | 435 (after 50 cycles) [c] | 66 |
| Bulk Sb | 0.02−1.5 | 1.4 | Sb: 100 | 330 | ~580 (after 160 cycles) [b] | 67 |

[a] The capacity value is calculated based on the mass of Sb-based composite; [b] The capacity value is calculated on the basis of Sb only; [c] The capacity value is calculated based on the mass of MSb (M = Cu, Sn, Bi, Ni, Zn, or Ge).

## References


1 T. Yang, T. Qian, M. Wang, X. Shen, N. Xu, Z. Sun and C. Yan, *Adv. Mater.*, 2016, **28**, 539.

2 S. Wang, L. Xia, L. Yu, L. Zhang, H. Wang and X. W. Lou, *Adv. Energy Mater.*, 2016, **6**, 1502217.

3 J. Song, Z. Yu, M. L. Gordin and D. Wang, *Nano Lett.*, 2016, **16**, 864.

4 Q. Ma, L. Wang, W. Xia, D. Jia and Z. Zhao, *Chem. Eur. J.*, 2016, **22**, 2339.
5 N.-L. Liu, S. Dutta, R. R. Salunkhe, T. Ahamad, S. M. Alshehri, Y. Yamauchi, C.-H. Hou and K. C. W. Wu, *Sci. Rep.*, 2016, **6**, 28847.
6 B. Li, F. Dai, Q. Xiao, L. Yang, J. Shen, C. Zhang and M. Cai, *Energy Environ. Sci.*, 2016, **9**, 102.
7 K. Zhang, X. Li, J. Liang, Y. Zhu, L. Hu, Q. Cheng, C. Guo, N. Lin and Y. Qian, *Electrochim. Acta*, 2015, **155**, 174.
8 J. Xu, M. Wang, N. P. Wickramaratne, M. Jaroniec, S. Dou and L. Dai, *Adv. Mater.*, 2015, **27**, 2042.
9 F. Zheng, Y. Yang and Q. Chen, *Nat. Commun.*, 2014, **5**, 5261.
10 T. Y. Ma, S. Dai, M. Jaroniec and S. Z. Qiao, *Angew. Chem., Int. Ed.*, 2014, **53**, 7281.
11 W. J. Lee, T. H. Hwang, J. O. Hwang, H. W. Kim, J. Lim, H. Y. Jeong, J. Shim, T. H. Han, J. Y. Kim, J. W. Choi and S. O. Kim, *Energy Environ. Sci.*, 2014, **7**, 621.
12 Z. Li, Z. Xu, X. Tan, H. Wang, C. M. B. Holt, T. Stephenson, B. C. Olsen and D. Mitlin, *Energy Environ. Sci.*, 2013, **6**, 871.
13 C. Lei, F. Han, D. Li, W.-C. Li, Q. Sun, X.-Q. Zhang and A.-H. Lu, *Nanoscale*, 2013, **5**, 1168.
14 Z.-H. Sheng, L. Shao, J.-J. Chen, W.-J. Bao, F.-B. Wang and X.-H. Xia, *ACS Nano*, 2011, **5**, 4350.
15 L. G. Bulusheva, A. V. Okotrub, A. G. Kurenya, H. Zhang, H. Zhang, X. Chen and H. Song, *Carbon*, 2011, **49**, 4013.
16 J. Liu, L. Yu, C. Wu, Y. Wen, K. Yin, F.-K. Chiang, R. Hu, J. Liu, L. Sun, L. Gu, J. Maier, Y. Yu and M. Zhu, *Nano Lett.*, 2017, **17**, 2034.
17 X. Zhang, P. Li, R. Zang, S. Wang, Y. Zhu, C. Li and G. Wang, *Chem. Asian J.*, 2017, **12**, 116.
18 L. Wang, C. Wang, N. Zhang, F. Li, F. Cheng and J. Chen, *ACS Energy Lett.*, 2017, **2**, 256.
19 G. J. Jung, Y. Lee, Y. S. Mun, H. Kim, J. Hur, T. Y. Kim, K. S. Suh, J. H. Kim, D. Lee, W. Choi and I. T. Kim, *J. Power Sources*, 2017, **340**, 393.
20 X. Xu, L. Si, X. Zhou, F. Tu, X. Zhu and J. Bao, *J. Power Sources*, 2017, **349**, 37.
21 A. Nie, L.-y. Gan, Y. Cheng, X. Tao, Y. Yuan, S. Sharifi-Asl, K. He, H. Asayesh-Ardakani, V. Vasiraju, J. Lu, F. Mashayek, R. Klie, S. Vaddiraju, U. Schwingenschlögl and R. Shahbazian-Yassar, *Adv. Funct. Mater.*, 2016, **26**, 543.
22 H. Gao, W. Zhou, J.-H. Jang and J. B. Goodenough, *Adv. Energy Mater.*, 2016, **6**, 1502130.
23 S. Liu, J. Feng, X. Bian, J. Liu and H. Xu, *Energy Environ. Sci.*, 2016, **9**, 1229.
24 N. Wang, Z. Bai, Y. Qian and J. Yang, *Adv. Mater.*, 2016, **28**, 4126.
25 Z. Liu, X.-Y. Yu, X. W. Lou and U. Paik, *Energy Environ. Sci.*, 2016, **9**, 2314.
26 X. Liu, Y. Du, X. Xu, X. Zhou, Z. Dai and J. Bao, *J. Phys. Chem. C*, 2016, **120**, 3214.
27 S. Qiu, X. Wu, L. Xiao, X. Ai, H. Yang and Y. Cao, *ACS Appl. Mater. Interfaces*, 2016, **8**, 1337.
28 W. Luo, P. Zhang, X. Wang, Q. Li, Y. Dong, J. Hua, L. Zhou and L. Mai, *J. Power Sources*, 2016, **304**, 340.
29 H.-Y. Lü, F. Wan, L.-H. Jiang, G. Wang and X.-L. Wu, *Part. Part. Syst. Charact.*, 2016, **33**, 204.
30 F. Wan, J.-Z. Guo, X.-H. Zhang, J.-P. Zhang, H.-Z. Sun, Q. Yan, D.-X. Han, L. Niu and X.-L. Wu, *ACS Appl. Mater. Interfaces*, 2016, **8**, 7790.
31 H. Lu, L. Wu, L. Xiao, X. Ai, H. Yang and Y. Cao, *Electrochim. Acta*, 2016, **190**, 402.
32 F. Wan, H.-Y. Lü, X.-H. Zhang, D.-H. Liu, J.-P. Zhang, X. He and X.-L. Wu, *J. Alloys Compd.*, 2016, **672**, 72.
33 N. Zhang, Y. Liu, Y. Lu, X. Han, F. Cheng and J. Chen, *Nano Res.*, 2015, **8**, 3384.
34 Y. Zhao and A. Manthiram, *Chem. Mater.*, 2015, **27**, 3096.
35 Y.-L. Ding, C. Wu, P. Kopold, P. A. van Aken, J. Maier and Y. Yu, *Small*, 2015, **11**, 6026.
36 H. Hou, M. Jing, Y. Yang, Y. Zhang, Y. Zhu, W. Song, X. Yang and X. Ji, *J. Mater. Chem. A*, 2015, **3**, 2971.
37 L. Liang, Y. Xu, C. Wang, L. Wen, Y. Fang, Y. Mi, M. Zhou, H. Zhao and Y. Lei, *Energy Environ. Sci.*, 2015,

**8**, 2954.
38 J. Duan, W. Zhang, C. Wu, Q. Fan, W. Zhang, X. Hu and Y. Huang, *Nano Energy*, 2015, **16**, 479.
39 H. Hou, M. Jing, Y. Yang, Y. Zhang, W. Song, X. Yang, J. Chen, Q. Chen and X. Ji, *J. Power Sources*, 2015, **284**, 227.
40 L. Hu, X. Zhu, Y. Du, Y. Li, X. Zhou and J. Bao, *Chem. Mater.*, 2015, **27**, 8138.
41 M. Wang, Z. Yang, J. Wang, W. Li, L. Gu and Y. Yu, *Small*, 2015, **11**, 5381.
42 L. Wu, H. Lu, L. Xiao, X. Ai, H. Yang and Y. Cao, *J. Mater. Chem. A*, 2015, **3**, 5708.
43 C. Yang, W. Li, Z. Yang, L. Gu and Y. Yu, *Nano Energy*, 2015, **18**, 12.
44 W. Zhang, Y. Liu, C. Chen, Z. Li, Y. Huang and X. Hu, *Small*, 2015, **11**, 3822.
45 M. Walter, R. Erni and M. V. Kovalenko, *Sci. Rep.*, 2015, **5**, 8418.
46 Y. Zhao and A. Manthiram, *Chem. Commun.*, 2015, **51**, 13205.
47 K. Li, D. Su, H. Liu and G. Wang, *Electrochim. Acta*, 2015, **177**, 304.
48 H. Hou, M. Jing, Y. Zhang, J. Chen, Z. Huang and X. Ji, *J. Mater. Chem. A*, 2015, **3**, 17549.
49 D.-H. Nam, K.-S. Hong, S.-J. Lim, M.-J. Kim and H.-S. Kwon, *Small*, 2015, **11**, 2885.
50 L. Ji, W. Zhou, V. Chabot, A. Yu and X. Xiao, *ACS Appl. Mater. Interfaces*, 2015, **7**, 24895.
51 J. Liu, Z. Yang, J. Wang, L. Gu, J. Maier and Y. Yu, *Nano Energy*, 2015, **16**, 389.
52 J.-H. Choi, C.-W. Ha, H.-Y. Choi, H.-C. Shin and S.-M. Lee, *Mater. Lett.*, 2015, **159**, 349.
53 X. Zhou, X. Liu, Y. Xu, Y. Liu, Z. Dai and J. Bao, *J. Phys. Chem. C*, 2014, **118**, 23527.
54 Y. N. Ko and Y. C. Kang, *Chem. Commun.*, 2014, **50**, 12322.
55 L. Wu, X. Hu, J. Qian, F. Pei, F. Wu, R. Mao, X. Ai, H. Yang and Y. Cao, *Energy Environ. Sci.*, 2014, **7**, 323.
56 Y. Zhang, J. Xie, T. Zhu, G. Cao, X. Zhao and S. Zhang, *J. Power Sources*, 2014, **247**, 204.
57 X. Zhou, Y. Zhong, M. Yang, M. Hu, J. Wei and Z. Zhou, *Chem. Commun.*, 2014, **50**, 12888.
58 M. He, K. Kravchyk, M. Walter and M. V. Kovalenko, *Nano Lett.*, 2014, **14**, 1255.
59 L. Ji, M. Gu, Y. Shao, X. Li, M. H. Engelhard, B. W. Arey, W. Wang, Z. Nie, J. Xiao, C. Wang, J.-G. Zhang and J. Liu, *Adv. Mater.*, 2014, **26**, 2901.
60 B. Farbod, K. Cui, W. P. Kalisvaart, M. Kupsta, B. Zahiri, A. Kohandehghan, E. M. Lotfabad, Z. Li, E. J. Luber and D. Mitlin, *ACS Nano*, 2014, **8**, 4415.
61 X. Zhou, Z. Dai, J. Bao and Y.-G. Guo, *J. Mater. Chem. A*, 2013, **1**, 13727.
62 D. Y. W. Yu, P. V. Prikhodchenko, C. W. Mason, S. K. Batabyal, J. Gun, S. Sladkevich, A. G. Medvedev and O. Lev, *Nat. Commun.*, 2013, **4**, 2922.
63 Y. Zhu, X. Han, Y. Xu, Y. Liu, S. Zheng, K. Xu, L. Hu and C. Wang, *ACS Nano*, 2013, **7**, 6378.
64 L. Wu, F. Pei, R. Mao, F. Wu, Y. Wu, J. Qian, Y. Cao, X. Ai and H. Yang, *Electrochim. Acta*, 2013, **87**, 41.
65 J. Qian, Y. Chen, L. Wu, Y. Cao, X. Ai and H. Yang, *Chem. Commun.*, 2012, **48**, 7070.
66 L. Xiao, Y. Cao, J. Xiao, W. Wang, L. Kovarik, Z. Nie and J. Liu, *Chem. Commun.*, 2012, **48**, 3321.
67 A. Darwiche, C. Marino, M. T. Sougrati, B. Fraisse, L. Stievano and L. Monconduit, *J. Am. Chem. Soc.*, 2012, **134**, 20805.